

Driver's braking behavior approaching pedestrian crossings: a parametric duration model of the speed reduction times

Francesco Bella* and Manuel Silvestri

Department of Engineering, Roma TRE University, Via Vito Volterra n. 62-00146 Rome, Italy

SUMMARY

The driver's braking behavior while approaching zebra crossings under different safety measures (curb extensions, parking restrictions, and advance yield markings) and without treatment (baseline condition) was examined. The speed reduction time was the variable used to describe the driver's behavior. Forty-two drivers drove a driving simulator on an urban scenario in which the baseline condition and the safety measures were implemented. The speed reduction time was modeled with a parametric duration model to compare the effects on driver's braking behavior of vehicle dynamic variables and different countermeasures. The parametric accelerated failure time duration model with a Weibull distribution identified that the vehicle dynamic variables and only the countermeasure curb extensions affected, in a statistically significant way, the driver's speed reduction time in response to a pedestrian crossing.

This result shows that the driver, because of the improved visibility of the pedestrian allowed by the curb extensions, was able to receive a clear information and better to adapt his approaching speed to yield to the pedestrian, avoiding abrupt maneuvers. This also means a reduction of likelihood of rear-end collision due to less aggressive braking. Copyright © 2016 John Wiley & Sons, Ltd.

KEY WORDS: driving simulator; road safety; pedestrian; driver's braking behavior; parametric duration model

1. INTRODUCTION

The pedestrians are one of the road user categories that is the most exposed to high-risk levels. Recent accident statistics report that more than each year 270,000 pedestrians lose their lives on the roads all around the world [1]. In the particular case of Italy, pedestrians constitute more than 16% of all road deaths and more than 21,000 are injured in traffic-related crashes [2]. More than 50% of accidents that involve pedestrians occur at pedestrian crossings [2]. In the literature, many issues that concern pedestrians are investigated. The main research area concerns the pedestrian behavior in urban areas and focuses especially on the route choice and the crossing behavior [e.g. 3, 4]. Interaction between pedestrians and vehicles has received notably less attention [4]; in particular, few studies of driver's behavior are available in the literature. However, it is generally agreed that pedestrian-vehicle crashes are associated with a lack of driver compliance, which drivers often fail to yield to the pedestrian [5], and that pedestrian safety at zebra crossings depends mainly on speed of the vehicle. With an increase in the speed, in fact, the probability of a vehicle-pedestrian conflict and a pedestrian fatality accident is higher [6–11].

Inducing in the driver an appropriate speed adaptation while approaching the zebra crossings through driver oriented countermeasures (i.e., that are aimed at modifying the driver's speed behavior) is expected to have great potential for improving pedestrian safety and for reducing abrupt maneuvers that could lead to a rear-end collisions.

*Correspondence to: Francesco Bella, Department of Engineering, Roma TRE University, Via Vito Volterra n. 62, 00146 Rome, Italy. E-mail: francesco.bella@uniroma3.it

In literature, some studies highlight positive effects of several driver oriented countermeasures (such as curb extensions, parking restrictions, advance yield markings, pedestrian-activated flashing beacons, and in-pavement warning lights) in terms of operating speed, number of drivers yield to the pedestrian, distance that the driver yields to the pedestrians [e.g. 12–15]. However, there are still no studies that assess the effectiveness of the countermeasures on the basis of the braking behavior induced in the drivers while approaching the pedestrian crossings.

The present study was aimed to examine the driver's braking behavior while approaching zebra crossings under different safety measures. More specifically, a configuration of zebra crossing without treatment (baseline condition) and three safety measures, such as curb extensions, parking restrictions, and advance yield markings that are characterized by low cost, simple installation and high potential effectiveness on driver behavior, were investigated. The speed reduction time, defined as the elapsed time between the initial speed value (i.e., the speed value when the driver releases the accelerator pedal or starts to brake in response to a pedestrian crossing) and the minimum speed value when the driver yields to the pedestrian, was the variable used to describe the driver's behavior. The width of the interval time taken by the driver to pass from the initial speed to the minimum speed highlights if the driver receives an information that is more or less clear about the pedestrian crossing and, therefore, if he can yield to the pedestrian with a gradual maneuver. In other words, a small speed reduction time reveals an inappropriate driver's braking behavior indicating that the driver needs to modify his speed in a short time in response to a crossing pedestrian, and therefore, he adopts abrupt maneuver. The speed reduction time was modeled by the use of a parametric duration model, also called "survival model" or "hazard-based duration model", to compare the effects on driver's braking behavior of vehicle dynamic variables and different countermeasures.

The study reported here was carried out within a larger research program to analyze how different conditions of vehicle-pedestrian interaction and safety measure at pedestrian crossings affect driver's behavior. The first results of this research program on the effects on driver's behavior of different driver-pedestrian interactions are reported in Bella and Silvestri [16]. For the overall aim of the research program, of which this study is a part, a driving simulator experiment, that allows risk avoidance for the experimenters and full control of the experimental conditions, was performed.

2. METHODOLOGY

2.1. Hazard-based duration model

A hazard-based duration model is a probabilistic method that is used for analyzing data in the form of time from a well-defined time origin until the occurrence of some particular event of an end-point [17]. Such modeling is a common topic in many areas including biomedical, engineering, and social sciences. In the transportation field, hazard-based duration models have been applied to study a number of time-related issues such as analyzing the critical factors that affect accident duration and developing accident duration prediction models [18–20], analyzing the crossing behavior of cyclist at signalized intersections [21], modeling the pedestrian behavior violator and risk exposure at signalized crosswalk [22, 23], studying the effects of the phone use on the driver reaction time in response to a crossing pedestrian [24, 25], predicting the pavement performance over the time [26], exploring the factors that affect airport security transit times [27], developing a subway operational incident delay model [28], developing a accident duration model with endogenous variable [29], modeling the duration of freeway and highway traffic incident [30–32], and investigating the traffic delay due to incident frequency, durations, and lanes blockage [33].

In this study, speed reduction time is the duration variable. The speed reduction time is a continuous random variable T with a cumulative distribution function and probability density function, $F(t)$ and $f(t)$, respectively; the first gives the probability that a driver ends to brake with a speed reduction time lower than t . Conversely, the survivor function $S(t)$ is the probability of a speed reduction time longer than that some specified time t .

$$F(t) = Pr(T < t) = 1 - Pr(T \geq t) = 1 - S(t) \quad (1)$$

The hazard function $h(t)$ gives the conditional failure rate. More specifically, $h(t)$ is the conditional probability that an event will end between time t and $t + dt$, given that the event has not ended up to time t [26].

$$h(t) = \lim_{\Delta t \rightarrow 0} \frac{Pr(t + \Delta t \geq T \geq t | T \geq t)}{\Delta t} = \frac{f(t)}{S(t)} \quad (2)$$

The proportional hazard and the accelerated failure time (AFT) models are two alternative parametric approaches that allow incorporating the influence of covariates on a hazard function. The proportional hazard model assumes that the hazard ratios are constant over the time. The AFT model, instead, allows the covariates to accelerate time in a baseline survivor function, which is the survivor function when all covariates are zero [34]. The AFT assumption allows a simple interpretation of results because the estimated parameters quantify the corresponding effect of a covariate on the mean survival time [24, 25]. Given these features, AFT models were applied in this study. In the AFT model, the natural logarithm of the speed reduction times, $\ln(T)$, is expressed as a linear function of explanatory variables, as follows:

$$\ln(T) = \beta X + \varepsilon \quad (3)$$

where X is a vector of explanatory variables, β is a vector of estimable parameters and ε is the error term. Following Washington [34], the survival function in the AFT model can be written as

$$S(t|\mathbf{X}) = S_0[t \exp(\beta \mathbf{X})], \quad (4)$$

which leads to the conditional hazard function

$$h(t|\mathbf{X}) = h_0[t \exp(\beta \mathbf{X})] \exp(\beta \mathbf{X}), \quad (5)$$

where h_0 and S_0 are the baseline hazard and the baseline survival function, respectively.

Equations (4) and (5) show the effect of the covariates on the speed reduction time: the explanatory variables accelerate or decelerate the elapsed time to reduce the speed to the minimum value during the yielding phase. In order to estimate the hazard and the survival function in a fully parametric setting, a distribution assumption of the duration variable is needed. Common distribution alternatives include Weibull, lognormal, exponential, gamma, log-logistic, and Gompertz distribution [34]. The drivers' speed reduction times in response to a crossing pedestrian are positive duration dependence events. In other words, with the increasing of the time, the probability that the driver is reducing his speed in response to a crossing pedestrian reasonably increases. Such physical phenomenon is consistent with the form of the lognormal, log-logistic, and Weibull survival functions. The selection of the appropriate distribution form was based on the probability plot method [35]. The Weibull distribution was assessed as the best fitting (the plotting showed that the best linear relationship between the speed survival times and the cumulative distribution function was for the Weibull function) and thus, selected as survival function for the following analysis. In addition, this function is suitable for modeling data with monotone hazard rates that either increase or decrease with time [24, 25], which is consistent with the present study.

The hazard function of the Weibull duration model is expressed as

$$h(t) = (\lambda P)(\lambda t)^{P-1} \quad (6)$$

and the survival function of the Weibull duration model is expressed as

$$S(t) = \exp(-\lambda t^P) \quad (7)$$

where λ and P are the location and the scale parameter, respectively. The location parameter, with the introduction of explanatory variables, has the following expression:

$$\lambda = \exp[-P(\beta_o + \beta_1 X_1 + \dots)] \quad (8)$$

where the β_i are the coefficients of the explanatory variables X_i . The final expression of the survival function of the Weibull duration model is the following:

$$S(t) = \exp\{-\exp[-P(\beta_o + \beta_1 X_1 + \dots)]t^P\} \quad (9)$$

The duration model as previously specified assumes that the individual observations are independent. However, in the present study, data were obtained from a repeated measures experiment. Therefore, the observations might be subjected to individual level of heterogeneity or frailty, which implies that data from an individual might be correlated [24, 25]. Without accounting for shared frailty or heterogeneities and potential correlations, the duration model would suffer from a specification error that could lead to erroneous inferences on the shape of the hazard function. In addition, the standard error estimates of the regression parameters might be underestimated and inferences from the estimated model might be misleading [24, 25]. To taking into account the effects of the repeated measures on the individual observations, two possible extensions of the AFT model could be used: Weibull regression model with clustered heterogeneity and Weibull regression model with shared frailty. Several previous studies applied the frailty type models in order to include the unobserved heterogeneity (i.e., frailty) with the aim of exploring the effect of freeway work zones on the non-recurrent traffic congestion [36], estimating the capacity reduction that is attributable to accidents in the opposite direction of accident [37] and developing models for the estimation of the temporal and spatial extent of congestion impact caused by accidents [38].

The model with clustered heterogeneity fits the standard duration model and then, adjusts the standard error estimates to account for the possible correlations induced by the repeated observations within individuals [39, 40].

Weibull regression model with shared frailty allows to taking into account the correlation among observations obtained from the same driver and maintains independence among observations across different drivers. The shared frailty model can be expressed by modifying the conditional hazard function (Equation (5)) as follows:

$$h_{ij}(t|\alpha_i) = \alpha_i h_{ij}(t) = \alpha_i h_0[t \exp(\beta \mathbf{X}_{ij})] \exp(\beta \mathbf{X}_{ij}) \quad (10)$$

where h_{ij} is the hazard function for the i th driver in the j th driving test and α_i is the shared frailty, which is assumed to be gamma or inverse-Gaussian distributed, with mean 1 and variance θ .

Weibull regression model with clustered heterogeneity and Weibull regression model with shared frailty were compared by the likelihood ratio statistics [34] and the Akaike's information criteria (AIC) [41] to identify the best fitting model. To determine the effects of explanatory variables, the exponents of the coefficients were calculated. The exponent of a coefficient provides an intuitive way of interpreting the results by translating to a percent change in the survival duration variable resulting from a unit increase for continuous explanatory variables and a change from zero to one for categorical or indicator variables [25].

2.2. Driving simulator experiment

The study was conducted using the advanced driving simulator of the Department of Engineering—Roma Tre University. Several studies have demonstrated that driving simulators are useful tools for the evaluation of the driver's behavior induced by the road configuration [42–53]. Moreover, driving simulators are ideal tools for studies whose field survey is made impossible by the implicit high risks that the experimenters would be subjected to and the difficulty of ensuring controlled experimentation conditions. In the literature, several driving simulator studies concerning the analysis of the effects of crosswalk treatments and the driver's perception of pedestrian are reported, showing the high potential and reliability of the use of driving simulators. Fisher and Garay-Vega [54] studied the driver performance for advance yield markings at marked mid-block crosswalks in multi-threat scenarios (two-way/four-lane road). Salamati *et al.* [55] analyzed the effects of three different pedestrian crosswalk treatments at the exit leg of multilane roundabouts. Gomez *et al.* [56] compared potential vehicle-pedestrian conflict under different types of pavement markings when a driver's view of the pedestrians in a crosswalk is obstructed. Garay-Vega *et al.* [57] evaluated the hazard anticipation skills of novice and experienced drivers when a potential threat (such as the presence of pedestrians at crosswalks) was experienced.

2.2.1. Road scenario

A two-lane urban road approximately 15 km long was implemented in the driving simulator. Sixteen mid-block zebra crossings with different configuration and vehicle-pedestrian interaction were included. These 16 zebra crossings were obtained combining the following:

- four pedestrian crossing configurations: the condition of no treatment (baseline condition) and three countermeasures (curb extensions, parking restrictions, and advanced yield markings);
- four conditions of vehicle-pedestrian interaction: absence of a pedestrian and three conditions with pedestrian starting the crossing when vehicle was approximately at 15 m, 35 m, and 55 m before zebra crossing to simulate a wide range of vehicle-pedestrian interactions that occurs at pedestrian crossings.

To ensure the same approaching condition, 16 signalized intersections were placed in advance of each zebra crossing. Each driver was obligated to stop at the signalized intersection, because of the red light that turned on when the driver was at approximately 100 m from the intersection. The distance between the signalized intersection and pedestrian crossing was equal to 400 m, which allowed the drivers to reach a congruous speed for the simulated urban scenario. The posted speed limit was 50 km/hour. The cross-section was 13 m wide formed by two 3.00 m wide lanes, two 2.00-m wide lateral parking lanes, and two 1.50-m wide sidewalks (Figure 1). This configuration was chosen because it is representative of most Italian urban areas, where parking is allowed until the zebra crossing. According to the Italian Highway Code [58], the strips of crosswalks were 1.50 m long, 0.50 m wide, and spaced 0.50 m from one another. In addition, two vertical signals that were related to the pedestrian crossings were placed: first, at the pedestrian crossing and, second, at 150 m in advance of it. This configuration represents the baseline condition, in other words, a typical pedestrian crossing without any treatment (Figure 1).

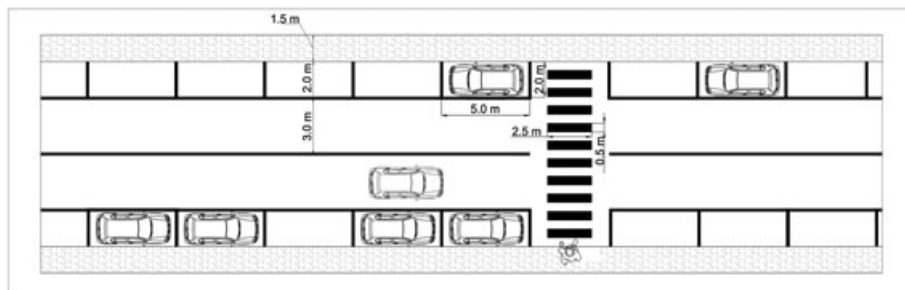


Figure 1. Baseline condition design.

In addition to the baseline condition, three countermeasures were implemented in the scenario: curb extensions, parking restrictions, and advanced yield markings.

The first (curb extensions) was designed according to the Road Design and Construction Standards [59]. As shown in Figure 2, curb extensions are an extension of the edge of the sidewalk and are commonly made along roads that are equipped with parking places on the sides of the lanes. The curb extends up to the line that separates the lane from parking stalls that are made on the side of the roadway. The effects that are expected from this safety countermeasure are to slow down the vehicles, reduce the pedestrian exposure and increase his visibility [60–62].

Parking restrictions are parking rules that are designed to not allow parking upstream of the zebra crossing, to improve pedestrian visibility. The presence of on-street parking, in fact, is associated with an increased risk of accidents [63, 64]. This countermeasure was designed following the Italian road design guidelines [65] and the Italian Highway Code [58]. The length of the upstream zone of the pedestrian crossing where parking is not allowed is a function of the stopping sight distance. According to the Italian road design guidelines, for a speed of 50 km/hour, the stopping sight distance is 55.3 m, and the parking restrictions length to allow the driver to see the pedestrian and react from that distance is 13.2 m (Figure 3).

Advanced yield markings consist of a series of triangular pavement markings that are placed across the travel lane and 15 m in advance of the zebra crossing. A “Yield Here to Pedestrian” vertical sign is also placed at the location of the markings. This countermeasure is aimed at improving the yielding compliance; it should alert the driver further upstream of the crosswalk to the possible presence of pedestrians and prompt the driver to yield [66–68]. The reference for the advanced yield markings was the Manual on Uniform Traffic Control Devices [69]. The triangular pavement markings have a base of 0.4 m, a height of 0.5 m, and are separated by 0.2 m from one another. Each pedestrian crossing is preceded by two parked cars on the right side of the driver, to reproduce the low visibility of a pedestrian (Figure 4).

With respect to the presence of pedestrian, the condition of pedestrian from right was considered; this condition is the most critical because of the following:

- the occlusion of the line of sight of an approaching vehicle due to the parking on the right, which does not allow the advanced detection of the pedestrian;
- pedestrian can reach the conflict point in a short time.

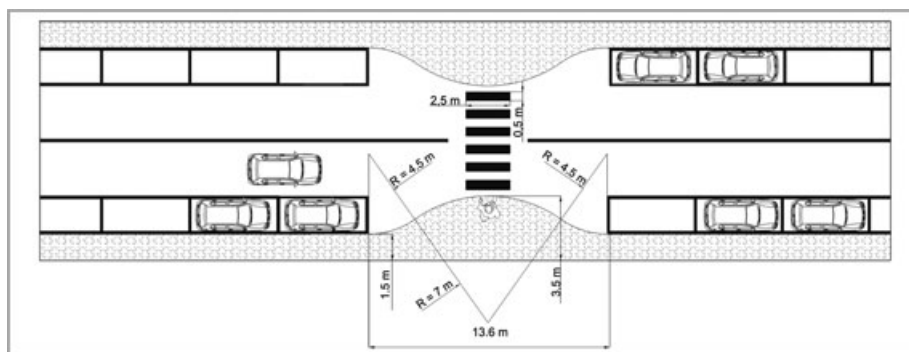


Figure 2. Curb extensions design.

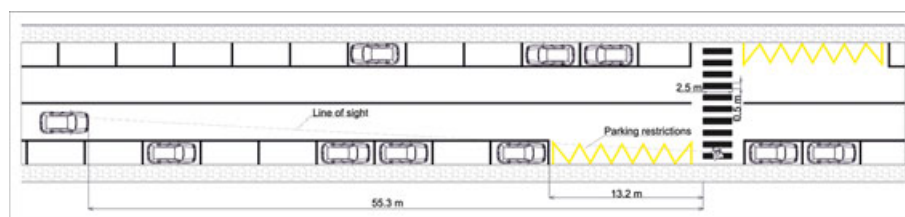


Figure 3. Parking restrictions design.

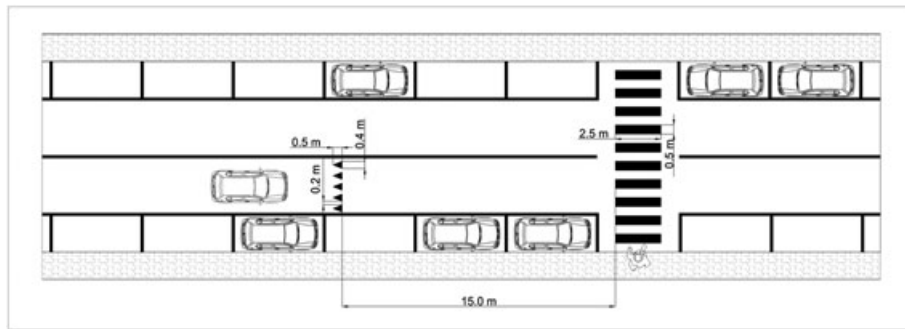


Figure 4. Advanced yield markings design.

To control for carry-over effects, three road scenarios that have a different sequence of the 16 combinations of zebra crossing-pedestrian (i.e., four pedestrian crossing configurations \times four conditions of vehicle-pedestrian interaction) were implemented in the driving simulator. Each scenario was driven by one of the three groups into which the participants were divided (see next section on participants).

2.2.2. Apparatus

The driving simulator of the Department of Engineering—Roma Tre University is an interactive fixed-base driving simulator. It was previously tested, calibrated, and validated [70–72] as a reliable tool for the study of the driver's speed behavior. The hardware interfaces (wheel, pedals, and gear lever) are installed on a real vehicle. The driving scene is projected onto three screens: one in front of the vehicle and one on either side, which provide a 135° field of view. The resolution of the visual scene is 1024×768 pixels with a refresh rate of 30 to 60 Hz. The system is also equipped with a sound system that reproduces the sounds of the engine. The simulator provides many parameters for describing the travel conditions (e.g., vehicle barycenter, relative position in relation to the road axis, local speed and acceleration, steering wheel rotation angle, pitching angle, and rolling angle). The data recording system acquired all of the parameters at spatial intervals of 2 m.

2.2.3. Procedure

The experiment was conducted with the free vehicle in its own driving lane. In the other driving lane, a slight amount of traffic was distributed to induce the driver to avoid driving into that lane. The simulated vehicle was a standard medium-class car with automatic gears. The participants were first briefed about the experiment and the use of the hardware interface (i.e., wheel and pedals and automatic gear) and then invited to filling in a form with personal data, years of driving experience, average annual distance driven. Before starting experimental drive, each participant performed a training drive at the driving simulator on a specific alignment with a length of approximately 5 km, to become familiar with the driving simulator. Participants encountered several traffic events including stop-sign intersections, overtaking a car, and crossing pedestrian at signalized intersection. After the training, participants drove one of the three road scenarios with a specific zebra crossing-pedestrian sequence. At the end of the road scenario, each participant filled in a questionnaire about the discomfort that was perceived during driving, to eliminate from the sample driving performed under anomalous conditions. This questionnaire consisted of five questions, with each question addressing a typed of discomfort: nausea, giddiness, daze, fatigue, and other. Each question could be answered by a score of 1–4 in proportion to the level of discomfort experienced: null, light, medium, and high. The null and light level for all five types of discomfort is considered to be the acceptable condition for driving. The last step was the filling in of a questionnaire about the perceived effectiveness of the countermeasures. This questionnaire consisted of three questions: the first was related to the effective influence perceived by the driver, the second (only for drivers that perceived an influence on their behavior) was related to the type of influence (slowing down, more willingness to yield, and more visibility of pedestrians), and the third related to the self-reported distance from the zebra crossing, where they modified their speed. For this last question, drivers could choose between the following values: less than 20 m, from 20 to 30 m, from 30 to 40 m, from 40 to 50 m, from 50 to 60 m, and higher than 60 m. Drivers were instructed to drive as they normally would in the real world.

2.2.4. Participants

Forty-two drivers (24 men and 18 women), whose ages ranged from 23 to 59 (average 29) and who had regular European driving licenses for at least three years were selected to perform the driving in the simulator. They were chosen from students, faculty and staff of the University, and volunteers from outside of the University. The drivers had no prior experience with the driving simulator and had an average annual driven distance on urban roads of at least 2500 km. The average number of years of driving experience was approximately nine. According to the questionnaire on perceived discomfort, all of the participants experienced null or light levels of discomfort. Thus, the sample used for the analysis consisted of all 42 drivers, which were divided into three groups; the three groups drove different scenarios, which were each characterized by a specific sequence of zebra-crossing pedestrian.

3. DATA PROCESSING

For the aim of the study, the drivers' braking behaviors while yielding to the pedestrian were analyzed. The speed profile of each driver when approaching a zebra crossing where a pedestrian started the crossing was plotted for the section of 150 m in advance of the pedestrian crossing. Overall, 504 speed profiles were analyzed. On the basis of the collected data, the following variables of the driver's braking behavior were determined (Figure 5).

- V_i : the driver's initial speed value, identified at the moment when the driver starts to decrease his speed, releasing the accelerator pedal or pressing the braking pedal;
- L_{V_i} : the distance from the zebra crossing where the initial speed value is located;
- V_{\min} : the driver's minimum speed value reached during the deceleration phase;
- $L_{V_{\min}}$: the distance from the zebra crossing where the minimum speed value is located;
- d_m : the average deceleration rate during the speed reduction phase from V_i to V_{\min} ; this variable is given by the following equation:

$$d_m = \frac{V_i^2 - V_{\min}^2}{2S} \quad (11)$$

where S is the distance between the points where the speed is equal to V_i and V_{\min} .

- speed reduction time: the elapsed time between the initial speed value (V_i) and the minimum speed value (V_{\min}).

Several events of failed yielding to pedestrian were also recorded: 11 for baseline condition, 6 for curb extensions, 17 for parking restrictions, and 8 for advanced yield markings. Thus, 462 observations of driver's braking behavior were used for the analysis. It should be noted that the size of this sample data is higher than those used in previous driving simulator studies for the development of hazard based duration models [24, 25]. Moreover, this number of data is consistent with several studies based on field observations and aimed to develop survival models [20, 22, 26].

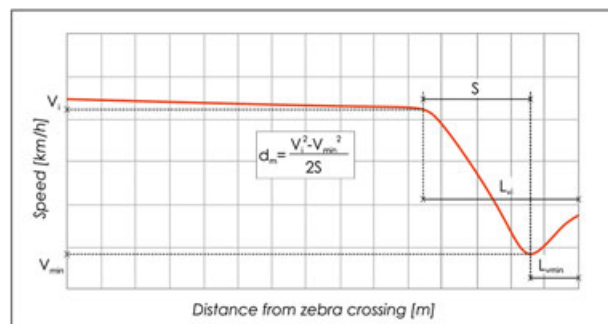


Figure 5. Variables of the driver's braking behavior.

4. DATA ANALYSIS AND RESULTS

The Table I shows the descriptive statistics of the continuous variables used in the Weibull AFT model and the speed reduction time.

The time to reduce the speed from the initial value to the minimum value was first tested and compared across the countermeasures by using the ANOVA test, to assess if the safety measures affect the driver's braking behavior while yielding to the pedestrian under different pedestrian crossing conditions. Bonferroni correction was used for multiple comparisons.

4.1. Speed reduction times

Drivers' speed reduction times measured from the initial speed to the minimum speed during the yielding phase are shown in Figure 6. ANOVA revealed that there was a significant main effect across the countermeasures ($F_{(3, 458)}=7.52, p=0.000$). The longer speed reduction time was reached when the curb extensions were present (4.34 seconds), which was statistically significantly longer than that in baseline condition (mean difference = 1.40 second, $p=0.000$), in parking restrictions (mean difference = 0.93 second, $p=0.020$), and in advanced yield markings (mean difference = 1.08 second, $p=0.003$). No other mean difference was statistically significant. Therefore, braking behavior is affected by the countermeasures; thus, to gain insight into the driver's braking behavior, the survival time of speed changes from the initial speed to the minimum speed was modeled using hazard-based duration models.

4.2. Hazard-based duration model

The speed reduction times from the initial speed to the minimum speed were modeled with the Weibull AFT, and two extensions of this model were tested; the Weibull AFT model with inverse-Gaussian shared frailty and the Weibull AFT model with clustered heterogeneity. The two models were compared with their likelihood ratio statistics and with the AIC test. The likelihood ratio statistics of the Weibull AFT model with shared frailty and with clustered heterogeneity was -216.83 and -222.23 , respectively, highlighting that the first was preferable. The AIC test also confirmed the

Table I. Descriptive statistics of the continuous variables of the Weibull accelerated failure time model and speed reduction time.

Variable	Mean Value	Standard deviation
V_i (m/s)	13.35	3.09
L_{V_i} (m)	54.79	21.27
V_{\min} (m/s)	3.66	2.14
$L_{V_{\min}}$ (m)	21.22	13.97
d_m (m/s ²)	2.99	1.75
Speed reduction time (s)	4.23	1.75

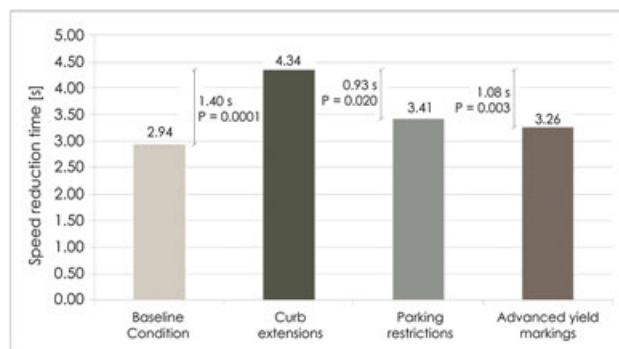


Figure 6. Effects of the safety measures on the speed reduction times.

previous result; for the shared frailty model, the AIC was 455.66, while for the clustered heterogeneity model was 466.47 (the model with the lower AIC is preferable). Thus, based on both likelihood ratio statistics and the AIC, the Weibull AFT model with shared frailty was the preferable for the speed reduction time of drivers in response to a crossing pedestrian, under different conditions of the zebra crossing.

An overall assessment of the goodness of fit for the Weibull AFT duration model with shared frailty can be showed with the representation of the cumulative hazard rate versus the Cox-Snell residuals, compared with a reference 45° line. In particular, the Cox-Snell residuals were determined from the model estimates and then used as time variable to generate an empirical estimate of the cumulative hazard function. The Figure 7 presents the Cox-Snell residuals for the Weibull AFT model with shared frailty. It should be noted that the plotted points follow quite well the reference straight line, suggesting that the predicted speed reduction time of drivers with the Weibull AFT model matches the observed data well.

The Table II shows the significant parameter estimates for the Weibull AFT model with shared frailty for the speed reduction times of drivers. The scale parameter p has an estimate value equal to 3.155, meaning that the survival probability of the speed reduction times decreased with the elapsed

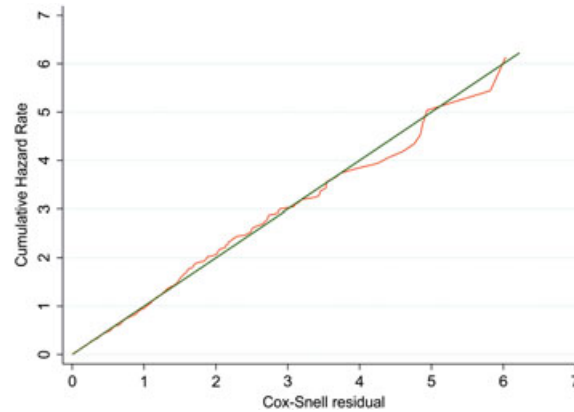


Figure 7. Cox-Snell residuals for the Weibull accelerated failure time model.

Table II. Variables for the Weibull accelerated failure time model with shared frailty.

Variable	Estimate	SE	z-statistic	p-value	Exp (β)	95% Conf. interval	
V_i (m/s)	0.049	0.009	5.55	0.000	1.05	0.032	0.067
L_{V_i} (m)	0.001	0.001	7.06	0.000	1.01	0.007	0.012
V_{\min} (m/s)	-0.099	0.009	-11.27	0.000	0.91	-0.116	-0.082
$L_{V_{\min}}$ (m)	-0.009	0.001	-6.65	0.000	0.99	-0.012	-0.007
d_m (m/s ²)	-0.274	0.016	16.87	0.000	0.76	0.242	0.306
<i>Pedestrian crossing condition</i>							
Baseline condition	-	-	-	-	-	-	-
Curb extensions	0.236	0.044	5.36	0.000	1.27	0.150	0.323
Parking restrictions	0.103	0.045	2.31	0.127	1.108	0.015	0.191
Advanced yield markings	0.107	0.043	2.48	0.079	1.113	0.022	0.191
Constant	1.250	0.087	14.27	0.000		1.078	1.421
p	3.155	0.134				2.903	3.429
Variance of inverse-Gaussian frailty, θ^a	0.130	0.064				0.049	0.339
Log-likelihood at convergence	-216.83						
Log-likelihood at zero	-496.24						
AIC	455.66						
Number of observations	462						
Number of groups	42						

^aLikelihood ratio test of θ : $\chi^2 = 11.00$, p -value < 0.000.

time. This implies that the probability of the driver response to a crossing pedestrian was increased with the elapsed time; in other words, the probability that the driver ends the braking maneuver, decreasing his speed from the initial value to the minimum value (this occurs in the speed reduction time), increases with the elapsed time. On average, in fact, the probability of decreasing the speed from V_i to V_{\min} after 4 seconds was approximately 4.4 times higher than that after 2 seconds (i.e., $(4/2)^{3.155-1}$). The effect on the probability of the scale parameter p higher than one ensures that the hypotheses concerning the speed reduction times (i.e., monotone hazard function and positive duration dependence) were consistent with the applied model. Concerning the appropriateness of inclusion of inverse-Gaussian shared frailty specification, the likelihood ratio test on the frailty parameter θ showed that effectively in the observation group the unobserved heterogeneity was present ($\chi^2 = 11.00$, $p = 0.000$).

The model identified that all the variables were statistically significant for the drivers' speed reduction times in response to a crossing pedestrian; the sign of all the coefficients was consistent with the effect on the speed reduction time. The coefficient of the initial speed was positive, which means that when the value of this variable increased, the time to reach the minimum speed (i.e., the speed reduction time) value also increased, because of the wider speed gradient. More specifically, for 1 m/second increase in the driver's initial speed, the time required to reach the minimum speed value was 5% longer ($\text{Exp}(\beta) = 1.05$). Also, the distance where the V_i is located (L_{V_i}) was positively associated with the speed reduction time; if the driver starts to brake farther from zebra crossing, in fact, he covers a greater distance to pass from the initial speed to the minimum speed, needing more time. With an increase of 1 m in L_{V_i} , the speed reduction time was 1% longer ($\text{Exp}(\beta) = 1.01$). The minimum speed value had a negative coefficient, meaning that with an increase of the V_{\min} , the speed reduction time decreased; this is consistent because if the minimum speed increases, the speed gradient is smaller, requiring less time. More specifically, for 1 m/second increase in the driver's minimum speed, the speed reduction time was 9% lower ($\text{Exp}(\beta) = 0.91$). The distance where the V_{\min} is located ($L_{V_{\min}}$) also had a negative coefficient; if the braking maneuver ends farther from zebra crossing, the distance to pass from the initial speed to the minimum speed is smaller, requiring less time. For 1 m increase in $L_{V_{\min}}$, the speed reduction time was 1% lower ($\text{Exp}(\beta) = 0.99$). The average deceleration rate was negatively associated with the survival speed reduction time; this is consistent because if the driver adopts a more aggressive maneuver to yield to the pedestrian, he passes from the initial speed to the minimum speed in less time. With an increase of 1 m/s^2 in the average deceleration rate, in fact, the speed reduction time was 24% lower ($\text{Exp}(\beta) = 0.76$).

Among the pedestrian crossing conditions, only the curb extensions were statistically significant and positively associated with the speed reduction time (mean difference = 1.62 second, $p = 0.000$). Compared with the baseline condition (6.06 seconds), the time to pass from the initial speed to the minimum speed (7.68 seconds) was 27% longer ($\text{Exp}(\beta) = 1.27$, see also Figure 10). Parking restrictions and advanced yield markings were also positively associated with the speed reduction time, but the differences with the baseline condition were not statistically significant (mean difference = 0.65 second, $p = 0.127$; mean difference = 0.69 second, $p = 0.079$, respectively). It should be noted that for the baseline condition a coefficient was not provided because it was the reference condition (i.e., the baseline condition had the shorter speed reduction time). A pairwise comparison with Bonferroni's correction among the safety measures was also performed; the results indicated that the speed reduction time for curb extensions (7.68 second) was statistically significantly longer than that for parking restrictions (mean difference = 0.97 second, $p = 0.014$) and for advanced yield markings (mean difference = 0.93 second, $p = 0.016$) (Figure 10). No other difference was statistically significant.

4.3. Outcome of the questionnaire

The Figure 8 shows the results of the questionnaire about the perceived effectiveness of the countermeasures, and for those who perceived effectiveness, the type of the effectiveness is also reported. The higher number of drivers that perceived effectiveness during the drive was reached for the curb extensions; for this countermeasure, almost all the sample of drivers (35 of 42, equal to 83%) perceived an effect on their driving behavior (Figure 8a). For the parking restrictions and advanced yield

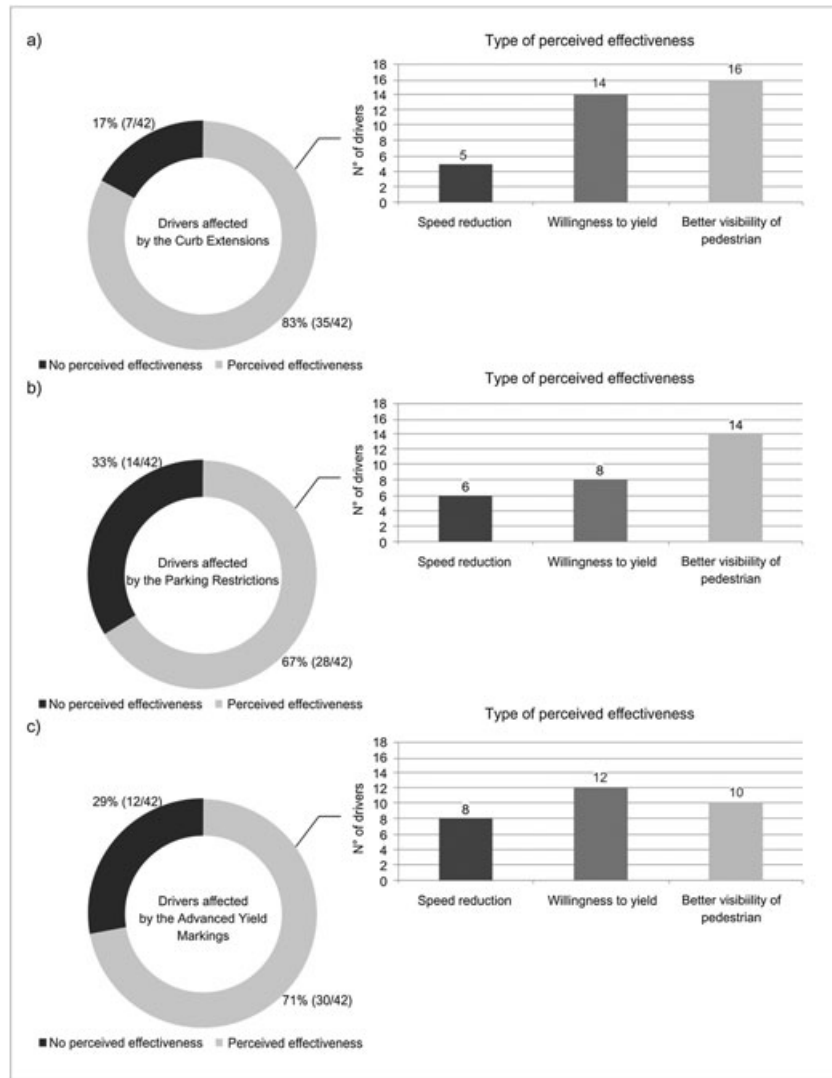


Figure 8. Drivers affected by the countermeasures and type of perceived effectiveness.

markings, the results were similar: 67% (28 of 42) when there were parking restrictions (Figure 8b) and 71% (30 of 42) when the treatment was the advanced yield markings (Figure 8c). A first comparison among the countermeasures, based on this result, indicates that the driver's behavior was more influenced when the curb extensions were present.

The drivers who experienced an effect during their drive also reported the type of the perceived effectiveness; for curb extensions and parking restrictions (Figure 8a and b), the drivers indicated the better visibility of pedestrian as the main effectiveness (16 of 35 and 14 of 28, respectively), while for the advanced yield markings, most of the drivers (12 of 30) indicated the willingness to yield as the main effectiveness (Figure 8c). Moreover, when curb extensions were present, several drivers indicated that they were also more willing to yield (14 of 35). For the three countermeasures, the effectiveness on the speed reduction was the less experienced by the drivers.

The Figure 9 shows the self-reported distance from zebra crossing where the driver started to modify the approaching speed. For the baseline condition, most drivers indicated that they modified the speed when they were too close to the zebra crossing (25 of 42, 59%). The higher distance intervals (from 40 to 50 m and from 50 to 60 m) were indicated by most drivers when the curb extensions were present (13 of 42 and 12 of 42, respectively, globally equal to 60%). This outcome is consistent with the

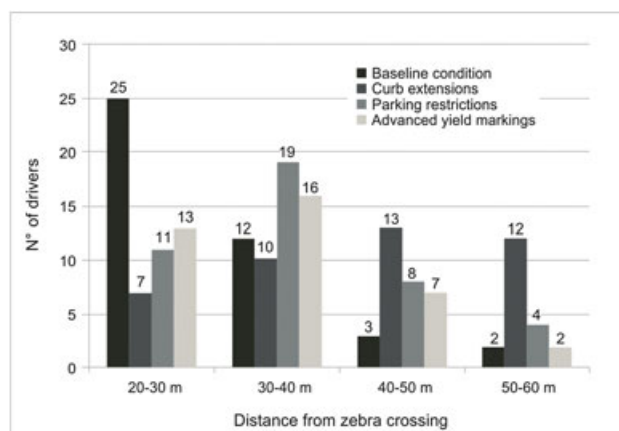


Figure 9. Self-reported distance from zebra crossing where the drivers modified their speed.

potential effectiveness of the countermeasure, which mainly allows the better visibility of the pedestrian. For the parking restrictions the intermediate distance interval (from 30 to 40 m) was selected by most of the drivers (19 of 42, 45%); this finding is also consistent with the aim of the countermeasure that of clearing the line-of-sight to the pedestrian crossing, but the outcome was less than that observed for the curb extensions. For the advanced yield markings, most of drivers (16 of 42, 38%) also selected the distance interval of 30 to 40 m; this result can be attributed to the markings and the vertical signs that advise the drivers in advance about the presence of the pedestrian crossing.

5. DISCUSSION

The use of the Weibull AFT model allowed a comparison of the driver's braking behavior in response to a crossing pedestrian, under different zebra crossing conditions. The representation of the drivers' braking patterns was possible by the plotting of the survival curves of the speed reduction time with the use of the several coefficients determined for the Weibull AFT model with shared frailty. The estimation of the survival curves was provided by the Equation (9), where the vector \mathbf{X} was represented by the driver's braking behavior variables, while the vector $\boldsymbol{\beta}$ was represented by the related coefficients. The survival curves for the several countermeasures were plotted by using the mean values of the continuous variable (Table I) and the coefficients in Table II.

For example, the survival probabilities of the speed reduction time for the parking restrictions and curb extensions after 3 seconds were respectively:

$$S(t = 3) = \exp \left\{ - \left[\exp(-3.155(1.250 + (0.049 * 13.35) + (0.001 * 54.79) + (-0.099 * 3.66) + (-0.009 * 21.22) + (-0.274 * 2.99) + 0.103)) \right] * 3^{3.155} \right\}$$

$$S(t = 3) = \exp \left\{ - \left[\exp(-3.155(1.250 + (0.049 * 13.35) + (0.001 * 54.79) + (-0.099 * 3.66) + (-0.009 * 21.22) + (-0.274 * 2.99) + 0.236)) \right] * 3^{3.155} \right\}$$

Using this method, the survival curve for each countermeasure was plotted (Figure 10).

As expected, the speed reduction time survival probability during the yielding phase decreases with the elapsed time (Figure 10). Thus, the probability that the driver completes the braking maneuver from V_i to V_{\min} increases with the elapsed time.

The survival curves for different pedestrian crossing conditions show that, for a fixed elapsed time, the higher speed reduction time survival probability was obtained for the curb extensions, while the lower survival probability was recorded for baseline condition. For example, after 4 seconds, the speed reduction time survival probability for curb extensions was 27.4%, while for the baseline condition was approximately 6.5%; for parking restrictions and advanced yield markings, the speed reduction time survival probability was 13.9% and 14.2%, respectively.

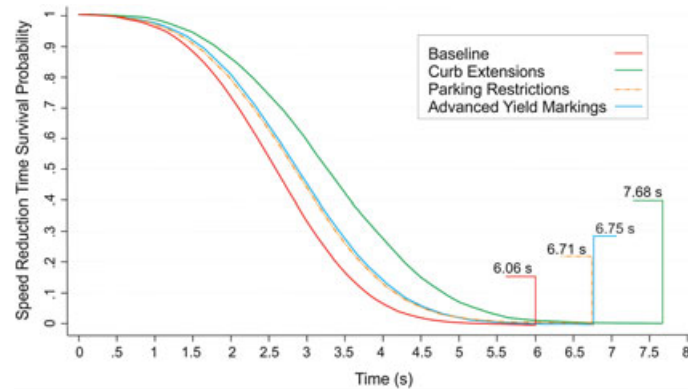


Figure 10. Survival curves of the speed reduction time for all the pedestrian crossing conditions and values of speed reduction times for null survival probability.

The event duration, that is, the speed reduction time (the time required to reduce the speed from the initial value to the minimum value), was 6.06 seconds for the baseline condition, while it was 1.62 second longer (statistically significant) for curb extensions, 0.65 second longer (not statistically significant) for parking restrictions, and 0.69 second longer (not statistically significant) for advanced yield markings.

It should be noted that speed reduction time values are representative of the same maneuver acted by the driver to yield to the pedestrian; this means that the longer values of the speed reduction times are linked to smoother yielding maneuver (i.e., the driver's braking behavior is less aggressive). The results of the Weibull AFT model showed that for the curb extensions, the longer time to pass from the initial speed to the minimum speed was required. This finding suggest that in this condition of pedestrian crossing, the drivers are able to start earlier the braking maneuver to yield to the pedestrian, and the consequence is that they undertake less deceleration rates. This is consistent with the findings of Randal [62], where pedestrian experienced a vehicle yielding sooner when the curb extensions were present. The improvement of the pedestrian visibility provided by the curb extensions allows the driver to advance the detection of the pedestrian, and thus, he has more time to brake and give way.

For the parking restrictions and the advanced yield markings, the speed reduction times were similar. The estimate coefficients were 0.103 and 0.107, respectively, indicating that the speed reduction time for the advanced yield markings was slightly longer. Although this result was not statistically significant, it can be attributed to the following reasons:

- presence of the pavement markings and the vertical sign that effectively warned the driver of the presence of the pedestrian, allowing him to start to brake slightly earlier than that in parking restrictions condition;
- absence of parked cars in advance of the zebra crossing in the parking restrictions condition, which improves the visibility of the pedestrian crossing, induces the perception of a wider lane and leads the driver to maintain the same speed for much time and, thus, to start the braking when he is closer to the zebra crossing.

For the baseline condition, the speed reduction time was the lower among all the countermeasures. This result was expected, because there were no improvements of the pedestrian crossing. In this condition, the driver was not able to advance the braking maneuver, and thus, he was forced to brake more abruptly.

6. CONCLUSIONS

The present study aimed to investigate the driver's braking behavior in response to a crossing pedestrian under different crosswalk treatments such as the curb extensions, the parking restrictions and the advanced yield markings. The time taken to reduce the speed from the initial value to the minimum value (called speed reduction time) was the variable used to describe the driver's braking behavior. This speed reduction time was modeled with the Weibull AFT model with shared frailty, to taking into account the possible

correlations due to the repeated measures and to compare the effects on driver's braking behavior of vehicle dynamic variables and different countermeasures. The hazard-based duration model identified that five vehicle dynamic variables (the initial speed and the distance from zebra crossing where the initial speed is located, the minimum speed and the distance from zebra crossing where the minimum speed is located and the average deceleration rate) and only the countermeasure curb extensions affected, in a statistically significant way, the driver's speed reduction time in response to a pedestrian crossing. The Weibull AFT model showed that for the curb extensions the drivers adopted a smoother maneuver to yield to the pedestrian. The speed reduction time for this countermeasure was longer (statistically significant) than those for the baseline condition and the other countermeasures. No other difference was statistically significant. These findings suggest that the driver, because of the improved visibility of the pedestrian allowed by the curb extensions, was able to receive a clear information on the presence of the pedestrian and better to adapt his approaching speed to yield to the pedestrian, avoiding abrupt maneuvers. The opportunity to not to brake hard during the approaching phase to the pedestrian crossing, also allows to avoid unexpected situations for the following vehicles and, thus, reduce the likelihood of rear-end collisions.

These results were also confirmed by the outcomes of the questionnaire on the countermeasures effectiveness. For the curb extensions, almost all the sample of drivers (over 80%) indicated that the curb extensions were effective and that the main effect was the better visibility of the pedestrian. Moreover, the drivers reported that when the curb extensions were present, they started to change their speed at a point farther from zebra crossing.

Further studies might examine combinations of treatments, such as curb extensions and advanced yield markings or parking restrictions and advanced yield markings. Such combinations of treatments remain inexpensive and easy to install and could determine additional effects on the driver's behavior than those found for the single treatment.

ACKNOWLEDGEMENTS

This research was financially supported by the Italian Ministry of Education, Research and Universities

REFERENCES

1. World Health Organization – WHO. Global status report on road safety. WHO Library Cataloguing in Publication Data, 2013.
2. Rapporto ACI - ISTAT sugli incidenti stradali 2013. [In italian]
3. Papadimitriou E, Yannis, G Golias J. A critical assessment of pedestrian behaviour models. *Transportation Research Part F* 2012; **12**: 242–255.
4. Papadimitriou E, Auberlet JM, Yannis G, Lassarre S. Challenges in simulation of pedestrians and motorised traffic. *Proceedings of Road Safety and Simulation International Conference RSS2013*; October 22–25, 2013 Rome, Italy.
5. Mitman MF, Cooper D DuBose B. Driver and pedestrian behavior at uncontrolled crosswalks in Tahoe Basin Recreation Area of California. *Transportation Research Record: Journal of the Transportation Research Board* 2010; **2198**: 23–31.
6. Pasanen E. Driving speeds and pedestrian safety; a mathematical model. Helsinki, University of Technology. Transport Engineering Publication 77.
7. Várhelyi A. Drivers' speed behaviour at a zebra crossing: a case study. *Accident Analysis and Prevention* 1998; **30**(6): 731–743.
8. Rosén E, Sander U. Pedestrian fatality risk as a function of car impact speed. *Accident Analysis and Prevention* 2009; **41**: 536–542.
9. Rosén E, Stigson H Sander U. Literature review of pedestrian fatality risk as a function of car impact speed. *Accident Analysis and Prevention* 2011; **43**: 25–33.
10. Tefft BC. Impact speed and a pedestrian's risk of severe injury or death. *Accident Analysis and Prevention* 2013; **50**: 871–878.
11. Kröyer HRG, Jonsson T Várhelyi A. Relative fatality risk curve to describe the effect of change in the impact speed on fatality risk of pedestrians struck by a motor vehicle. *Accident Analysis and Prevention* 2014; **62**: 143–152.
12. Hakkert AS, Gitelman V, Ben-Shabat E. An evaluation of crosswalk warning systems: effects on pedestrian and vehicle behaviour. *Transportation Research Part F* 2002; **5**(4): 275–292.
13. Fitzpatrick K, Turner S, Brewer M. Improving pedestrian safety at unsignalized crossings. Transportation Research Board 2006; NCHRP Report 562. Washington, D.C.

14. Zegeer CV, Bushell M. Pedestrian crash trends and potential countermeasures from around the world. *Accident Analysis and Prevention* 2012; **44**: 3–11.
15. Pulugurtha SS, Vasudevan V, Nambisan SS, Dangeti MR. Evaluating effectiveness of infrastructure-based countermeasures for pedestrian safety. *Transportation Research Record: Journal of the Transportation Research Board* 2012; **2229**: 100–109.
16. Bella F, Silvestri M. Effects of safety measures on driver's speed behavior at pedestrian crossings. *Accident Analysis and Prevention* 2015; **83**: 111–124. DOI:10.1016/j.aap.2015.07.016.
17. Collett D. *Modeling Survival Data in Medical Research* Chapman & Hall/CRC 2nd ed., Inc.: Boca Raton, FL, 2003.
18. Chung Y. Development of an accident duration prediction model on the Korean freeway systems. *Accident Analysis and Prevention* 2010; **42**(1): 282–289.
19. Chung Y, Walubita LF Choi K. Modeling accident duration and its mitigation strategies on south Korean freeway systems transportation research record. *Journal of the Transportation Research Board* 2010; **2178**: 49–57.
20. Hojati AT, Ferreira L, Washington S, Charles P Shobeirinejad A. Modeling total duration of traffic incidents including incident detection and recovery time. *Accident Analysis and Prevention* 2014; **71**: 296–305.
21. Yang X, Huan M, Abdel-Aty M, Peng Y Gao Z. A hazard-based duration model for analyzing crossing behavior of cyclists and electric bike riders at signalized intersections. *Accident Analysis and Prevention* 2015; **74**: 33–41.
22. Guo H, Gao Z, Yang X Jiang X. Modeling pedestrian violation behavior at signalized crosswalk in China: a hazards – based duration approach. *Traffic Injury Prevention* 2011; **12**: 96–103.
23. Tiwari G, Bangdiwala S, Saraswat A Gaurav S. Survival analysis: pedestrian risk exposure at signalized intersections. *Transport Research Part F* 2007; **10**: 77–89.
24. Haque MM, Washington S. A parametric duration model of the reaction times of drivers distracted by mobile phone conversation. *Accident Analysis and Prevention* 2014; **62**: 42–53.
25. Haque MM, Washington S. The impact of mobile phone distraction on the braking behavior of young drivers: a hazard based duration model. *Transport Research Part C* 2015; **50**: 13–27.
26. Anastasopoulos P, Mannering F. Analysis of pavement overlay and replacement performance using random parameters hazard-based duration models. *Journal of Infrastructure System* 2015; **21**(1): . DOI:10.1061/(ASCE)IS.1943-555X.0000208.
27. Hainen AM, Remias SM, Bullock DM Mannering FL. A hazard-based analysis of airport security transit times. *Journal of Air Transport Management* 2013; **32**: 32–38.
28. Weng J, Zheng Y, Yan X Meng Q. Development of a subway operation incident delay model using accelerated failure time approaches. *Accident Analysis and Prevention* 2014; **73**: 12–19.
29. Chung YS, Chiou YC Lin CH. Simultaneous equation modeling of freeway accident duration and lanes blocked. *Analytic Methods in Accident Research* 2015; **7**: 16–28.
30. Hojati AT, Ferreira L, Washington S Charles P. Hazard based models for freeway traffic incident duration. *Accident Analysis and Prevention* 2013; **52**: 171–181.
31. Junhua W, Haozhe C Shi Q. Estimating freeway incident duration using accelerated failure time modeling. *Safety Science* 2013; **54**: 43–50.
32. Nam D, Mannering F. An exploratory hazard – based analysis of highway incident duration. *Transportation Research Part A* 2000; **34**: 85–102.
33. Qi YG, Teng HH Martinelli DR. An investigation of incident frequency, duration and lanes blockage for determining traffic delay. *Journal of Advanced Transportation* 2009; **43**: 275–299.
34. Washington SP, Karlaftis MG Mannering FL. *Statistical and Econometric Methods for Transportation Data Analysis* (Second edn) Chapman and Hall/CRC, Inc.: Boca Raton, FL, 2011.
35. Lee E-T, Wang J-V. *Statistical Methods for Survival Data Analysis*. Third edn. *Wiley Series in Probability and Statistics* 2003.
36. Chung Y. Assessment of non-recurrent traffic congestion caused by freeway work zones and its statistical analysis with unobserved heterogeneity. *Transport Policy* 2011; **18**: 587–594.
37. Chung Y, Recker W-W. Spatiotemporal analysis of traffic congestion caused by rubbernecking at freeway accidents. *Intelligent Transportation Systems* 2013; **14**: 1416–1422.
38. Chung Y, Recker W-W. Frailty models for the estimation of spatiotemporally maximum congested impact information on freeway accidents. *Intelligent Transportation Systems* 2015; **16**: 2104–2112.
39. Cleves M, William G, Gutierrez RG Marchenko Y. *An Introduction to Survival Analysis Using States*. In *Stata Press* (second edn) College Station, Texas, 2008.
40. McGilchrist CA, Aisbett CW. Regression with frailty in survival analysis. *Biometrics* 1991; **47**: 461–466.
41. Akaike H. *Information theory and an extension of the maximum likelihood principle*. *Second international symposium of information theory* Budapest: Akademiai Kiado, 1973 267–281.
42. Bella F. New model to estimate speed differential in tangent–curve transition. *Advances in Transportation Studies an international Journal* 2008; **15**: 27–36. DOI:10.4399/97888548186823.
43. Bella F. Driver perception of roadside configurations on two-lane rural roads: Effects on speed and lateral placement. *Accident Analysis and Prevention* 2013; **50**: 251–262. DOI:10.1016/j.aap.2012.04.015.
44. Bella F. Driver performance approaching and departing curves: driving simulator study. *Traffic Injury Prevention* 2014; **15**: 310–318. DOI:10.1080/15389588.2013.813022.

45. Bella F. Operating speeds from driving simulator tests for road safety evaluation. *Journal of Transportation Safety & Security* 2014; **6**(3): 220–234. DOI:10.1080/19439962.2013.856984.
46. Bella F. Driver perception hypothesis: driving simulator study. *Transportation Research Part F*. Elsevier Ltd: Amsterdam, 2014; **24**: 183–196. DOI:10.1016/j.trf.2014.04.007.
47. Rosey F, Auberlet JM, Bertrand J Plainchault P. Impact of perceptual treatments on lateral control during driving on crest vertical curves: a driving simulator study. *Accident Analysis and Prevention* 2008; **40**: 1513–1523.
48. Bella F. How traffic conditions affect driver behavior in passing maneuver. *Advanced in Transportation Studies International Journal* 2011; (Spec. Issue): 113–126. DOI:10.4399/978885484657911.
49. Daniels S, Vanrie J, Dreesen A Brijs T. Additional road markings as an indication of speed limits: results of a field experiment and a driving simulator study. *Accident Analysis and Prevention* 2010; **42**: 953–960.
50. Jamson S, Lai F, Jamson H. Driving simulators for robust comparisons: a case study evaluating road safety engineering treatments. *Accident Analysis and Prevention*. Elsevier Ltd, 2010; **42**: 961–971.
51. Bella F, Calvi A. Effects of simulated day and night driving on the speed differential in tangent–curve transition: a pilot study using driving simulator. *Traffic Injury Prevention* 2013; **14**(4): 413–423. DOI:10.1080/15389588.2012.716880.
52. Bella F, Calvi A D'Amico F. Analysis of driver speeds under night driving conditions using a driving simulator. *Journal of Safety Research* 2014; **49**: 45–52. DOI:10.1016/j.jsr.2014.02.007.
53. Ariën C, Brijs K, Brijs T, *et al*. Does the effect of traffic calming measures endure overtime? – A simulator study on the influence of gates. *Transportation Research Part F* 2014; **22**: 63–75.
54. Fisher D, Garay – Vega L. Advanced yield markings and drivers' performance in response to multiple – threat scenarios at mid – block crosswalks. *Accident Analysis and Prevention* 2012; **44**: 35–41.
55. Salamati K, Schroeder B, Roupail NM, Cunningham C, Zhang Y Kaber D. Simulator study of driver responses to pedestrian treatments at multilane roundabouts. *Transportation Research Record: Journal of the Transportation Research Board* 2012; **2312**: 67–75.
56. Gomez RA, Samuel S, Gerardino LR, *et al*. Do advance yield markings increase safe driver behaviors at unsignalized, marked midblock crosswalks: driving simulator study. *Transportation Research Record: Journal of the Transportation Research Board* 2011; **2264**: 27–33.
57. Garay-Vega L, Fisher DL Pollatsek A. Hazard anticipation of novice and experienced drivers empirical evaluation on a driving simulator in daytime and nighttime conditions. *Transportation Research Record: Journal of the Transportation Research Board* **2007**; 2009: 1–7.
58. Ministry of Infrastructures and Transports. Nuovo codice della strada, D.L. 30 aprile 1992 n.285 e successive modificazioni. Gazzetta Ufficiale della Repubblica Italiana n. 114. (In Italian)
59. Washington County Department of Land Use and Transportation. Road design and construction standards 2011; Standard Details.
60. Macbeth A. Balliol Street Traffic Calming. Proceedings from 21 papers 1995; Ontario Traffic Conference.
61. Hawley L, Henson C, Hulse A Brindle R. Towards traffic calming: a Practitioners' manual of implemented local area traffic management and blackspot devices. *Federal Office of Road Safety* 1992; **126**. Canberra, Australian Capital Territory, Australia.
62. Randal SJ. Pedestrian safety impacts of curb extensions: a case study. Federal Highway Administration 2005; report No. FHWA-OR-DF-06-01.
63. Greibe P. Accident prediction models for urban roads. *Accident Analysis and Prevention* 2003; **35**: 273–285.
64. Edquist J, Rudin–Brown CM, Lenném MG. The effects of on-street parking and road environment visual complexity on travel speed and reaction time. *Accident Analysis and Prevention* 2012; **45**: 759–765.
65. Ministry of Infrastructures and Transports. Decreto Ministeriale del 5/11/2001 Norme funzionali e geometriche per la costruzione delle strade. Istituto Poligrafico dello Stato, Roma (in Italian).
66. Van Houten R, Malenfant JEL, McCusker D. Advance yield markings reduce motor vehicle/pedestrian conflicts at multilane crosswalks with an uncontrolled approach. *Transportation Research Record: Journal of the Transportation Research Board* 2001; **1773**: 69–74.
67. Van Houten R, McCusker D, Huybers S, Malenfant JEL, Rice-Smith D. Advance yield markings and fluorescent yellow-green RA-4 signs at crosswalks with uncontrolled approaches. *Transportation Research Record: Journal of the Transportation Research Board* 2002; **1818**: 119–124.
68. Samuel S, Romoser MRE, Gerardino LR, *et al*. Of advance yield markings and symbolic signs on vehicle–pedestrian conflicts: field evaluation. *Transportation Research Record: Journal of the Transportation Research Board* 2013; **2393**: 139–146.
69. Federal Highway Administration–FHWA. Manual on uniform traffic control devices with revision of 1 and 2. U.S. Department of transportation, federal highway administration, 2012.
70. Bella F. Validation of a driving simulator for work zone design. *Transportation Research Record: Journal of the Transportation Research Board* 2005; **1937**: 136–144. DOI:10.3141/1937-19.
71. Bella, F. Driving simulator for speed research on two-lane rural roads. *Accident Analysis and Prevention* 2008; **40**: 1078–1087. DOI:10.1016/j.aap.2007.10.015.
72. Bella F, Garcia A, Solves F, Romero M. Driving simulator validation for deceleration lane design. Compendium of Papers CD-ROM 86th annual meeting of the transportation research board 2007. Washington, DC. paper 07-0894